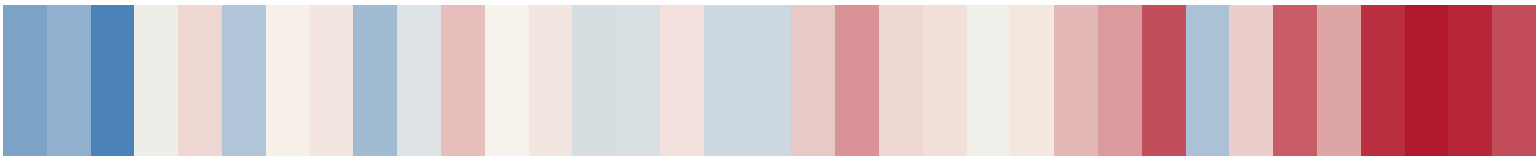
Morocco Climate and Economy Observatory
Climate risks, economy and financial stability

ECONOMIC AND CLIMATE BRIEF

Climate, economy and financial stability in Morocco

Situation at the end of September 2026



Temperature stripes: annual mean anomaly of the national temperature relative to 1991–2020, from 1991 to 2025 (blue: colder; red: warmer). Source: Open-Meteo (ERA5 reanalysis), Observatory calculations.

Author
Imad El Khlifi

Data
Open-Meteo (ERA5 reanalysis, forecasts, CAMS, Météo-France, ECMWF SEAS5); World Bank, World Development Indicators; Ministry of Equipment and Water (maadi-alna.ma); Observatory composite indices.

Latest complete climate month
September 2026

Site data last updated
23 October 2026

Online
observatoire-climat-maroc.pages.dev

Document produced automatically from the data published by the Observatory. Independent research site with no official status; this document is not investment advice. The statistical relationships presented are associations or predictive precedence and should not be read as causal effects.

Key points

- **Temperatures.** In September 2026, the national mean temperature anomaly reached +3.3 °C relative to the 1991–2020 normal, the warmest September since 1991. Over 1991–2025, 21 years out of 35 were warmer than normal; the mean anomaly rose from −0.37 °C in 1991–2000 to +0.82 °C in 2016–2025.
- **Drought.** The national SPEI-3 index stands at −1.11 (moderate drought) and the month's rainfall was 49 % of normal. Six regions out of 12 are in severe or extreme drought; the largest deficit is in Fez-Meknes (SPEI-3 of −3.12).
- **Farming season.** Since 1 September, an average of 26 mm of rain has fallen, 93 % of the normal for the same date (18 October 2026). The start of the season is close to normal.
- **Dams.** National dam filling stands at 65.9 % on 19 October 2026, about 11.2 billion m^3.
- **Climate risk.** The climate risk index (CRI) reached 100.0 in 2025, the maximum of the reference period. About 46 % of this value comes from the atypical deviation component, which treats a very wet year like a very dry one; the variant based on the first component alone stands at 80.9.
- **Financial stress.** The financial stress index (FSI) stands at 50.0 in 2025, a level rated normal relative to its historical distribution.
- **Forecast.** For 2026, the retained model (the naive model, lowest out-of-sample error) gives an FSI of 50.0, with an empirical interval of [32.5; 66.5]. None of the models using climate information beats this benchmark on the evaluation sample.

Temperature anomaly, September 2026
+3.3 °C
ref. 1991–2020
Open-Meteo (ERA5)

National SPEI-3 drought
−1.11
moderate drought
Open-Meteo (ERA5)

Climate risk index, 2025
100.0
level: exceptional
Scale 0–100

Financial stress index, 2025
50.0
level: normal
Scale 0–100

Purpose and sources

This brief presents the indicators tracked by the Morocco Climate and Economy Observatory as of the latest data update (23 October 2026). It brings together three sets of information: monthly climate indicators computed for the twelve regions from the ERA5 reanalysis, distributed through the Open-Meteo historical archive; two annual composite indices, one of climate risk (CRI) and one of financial stress (FSI), over 1998–2025; and estimation and forecasting results linking these two indices. The construction of the indices is presented in El Khlifi et al. (2026). Indicator definitions are given in the glossary at the end of the document.

1 Recent climate conditions

1.1 Temperatures

Figure 1 traces the annual anomaly of the national mean temperature. The series shows gradual warming: the mean anomaly of the last decade (+0.82 °C) is well above that of the first (−0.37 °C), and the warmest year of the period is 2023 (+1.47 °C). September 2026 extends this trend: at +3.3 °C,

it is the warmest September since 1991. The largest regional anomaly of the month was recorded in Marrakesh-Safi (+6.0 °C).

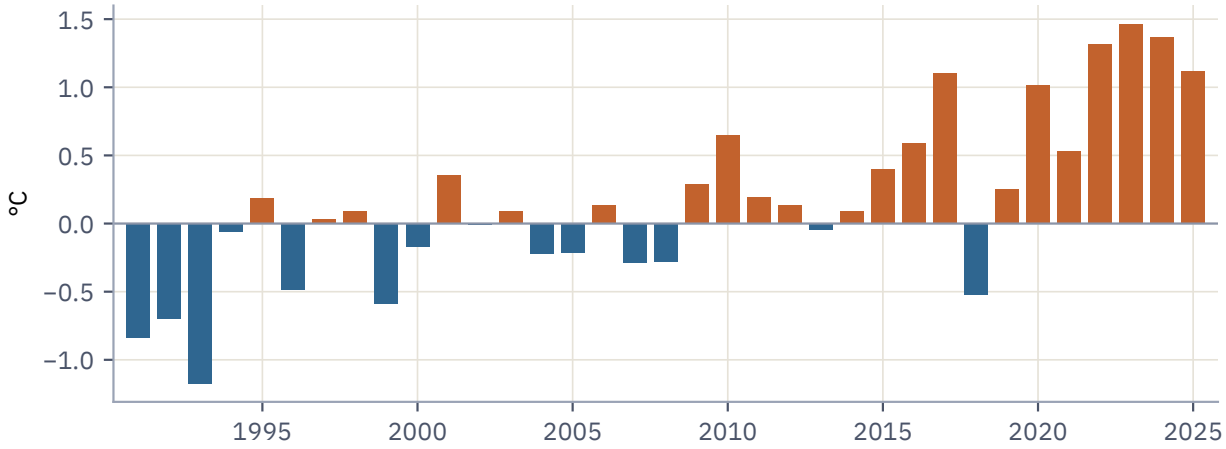


Figure 1: Annual anomaly of the national mean temperature relative to 1991–2020 (°C)
Complete years only. Unweighted mean of regional points. Source: Open-Meteo (ERA5 reanalysis), Observatory calculations.

1.2 Drought

The Standardised Precipitation Evapotranspiration Index (SPEI; Vicente-Serrano et al., 2010) measures the departure of the water balance (precipitation minus reference evapotranspiration) from its usual distribution for the same month. Over three months (SPEI-3), it reflects soil moisture and rain-fed farming; over twelve months (SPEI-12), water resources. At the end of September 2026, the national SPEI-3 is −1.11 and SPEI-12 is 0.76. The gap between the two horizons points to a recent deficit following a wetter period.

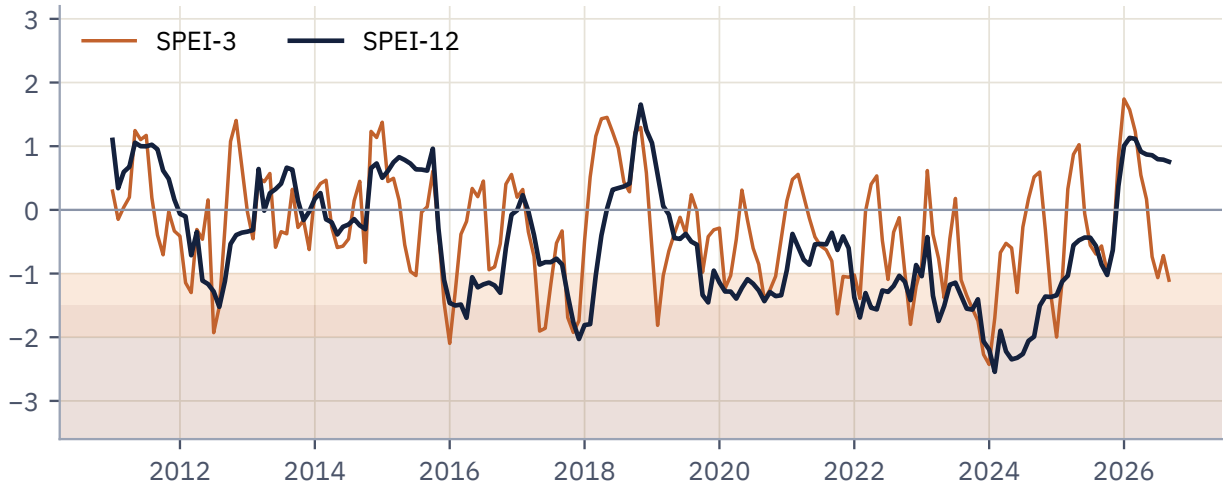


Figure 2: SPEI-3 and SPEI-12, national mean
Coloured bands: moderate (−1), severe (−1.5) and extreme (−2) drought thresholds. In summer, rainfall totals are small and short-term SPEI is less informative. Source: Open-Meteo (ERA5 reanalysis), Observatory calculations.

1.3 Regional situation

The situation varies across regions (figure 3 and table 1). Six regions out of 12 are in severe or extreme drought: Fez-Meknes, Laayoune-Sakia El Hamra, Guelmim-Oued Noun, Oriental, Tanger-Tetouan-Al Hoceima, Beni Mellal-Khenifra. At the other end, Casablanca-Settat has the highest SPEI-3 (0.69). Regional values are computed at each region's representative point (its capital) rather than averaged over its area; they should be read as indications of local trends.

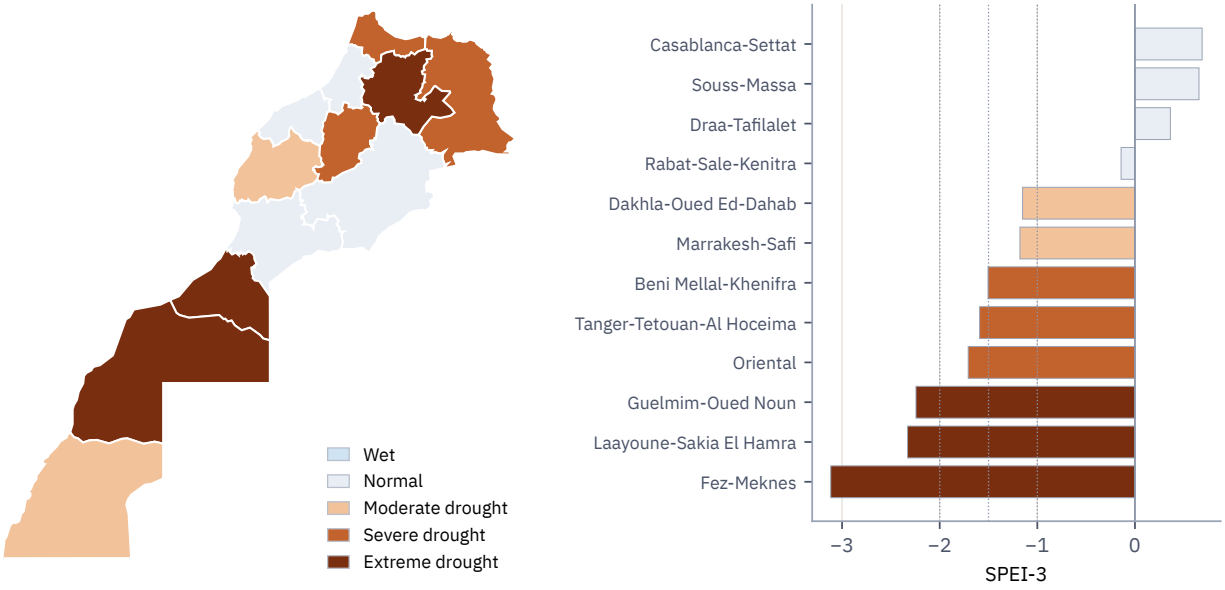


Figure 3: SPEI-3 drought by region, September 2026

Regional boundaries: © OpenStreetMap contributors (ODbL). Data source: Open-Meteo (ERA5 reanalysis), Observatory calculations.

Table 1: Regional climate indicators, September 2026

Region	SPEI-3	SPEI-12	Temp. anomaly (°C)	Rainfall (% normal)	Hot days	Drought (SPEI-3)
Fez-Meknes	−3.12	0.58	+4.6	7	15	extreme
Laayoune-Sakia El Hamra	−2.33	−0.11	+3.6	112	17	extreme
Guelmim-Oued Noun	−2.24	0.08	+5.4	137	17	extreme
Oriental	−1.71	−1.96	+3.0	36	9	severe
Tanger-Tetouan-Al Hoceima	−1.59	1.79	+2.8	6	13	severe
Beni Mellal-Khenifra	−1.51	1.17	+3.8	28	11	severe
Marrakesh-Safi	−1.18	1.86	+6.0	81	17	moderate
Dakhla-Oued Ed-Dahab	−1.15	−0.02	+1.1	15	8	moderate
Rabat-Sale-Kenitra	−0.14	2.08	+2.5	15	10	normal
Draa-Tafilalet	0.36	0.45	+0.9	100	5	normal
Souss-Massa	0.66	0.86	+2.6	41	12	normal
Casablanca-Settat	0.69	2.31	+2.9	10	10	normal

Hot days: days when the maximum temperature exceeds the 90th percentile of the same month over 1991–2020. Regions sorted from lowest to highest SPEI-3.

2 Water and heat through the year

2.1 Farming season rainfall 2026/27

The farming season starts on 1 September. As of 18 October 2026, average cumulative rainfall reached 26 mm, against 28 mm on average at the same date over the 1991/92–2019/20 seasons, i.e. 93 % of normal. The start of the season is close to normal. This start of season ranks 19 among the driest of 36 seasons since 1991. For reference, the normal for a full season is 295 mm, and the driest season of the period, 2004/05, totalled only 185 mm. The regions furthest behind are Souss-Massa (20 %), Rabat-Sale-Kenitra (30 %), Tanger-Tetouan-Al Hoceima (43 %) (table 2).

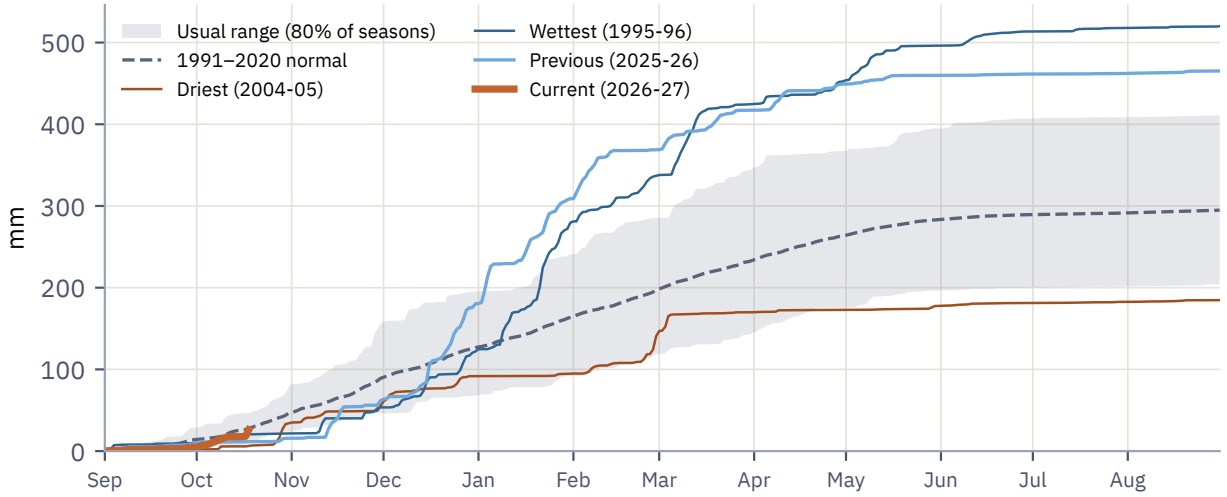


Figure 4: Cumulative rainfall since 1 September, national mean (mm)

Grey band: 80 % of the 1991/92–2019/20 seasons at the same date (10th to 90th percentile). Unweighted mean of regional points. Source: Open-Meteo (ERA5 reanalysis), Observatory calculations.

Table 2: Current season rainfall by region

Region	Total (mm)	Normal to date (mm)	% of normal	Rank (driest)
Souss-Massa	3	14	20	13 / 36
Rabat-Sale-Kenitra	11	35	30	6 / 36
Tanger-Tetouan-Al Hoceima	25	58	43	9 / 36
Beni Mellal-Khenifra	29	47	62	13 / 36
Laayoune-Sakia El Hamra	6	7	76	22 / 36
Oriental	31	39	79	18 / 36
Casablanca-Settat	22	24	94	21 / 36
Fez-Meknes	54	56	96	22 / 36
Dakhla-Oued Ed-Dahab	7	7	103	26 / 36
Guelmim-Oued Noun	8	7	118	26 / 36
Marrakesh-Safi	37	22	164	30 / 36
Draa-Tafilalet	81	18	440	34 / 36

Regions sorted from the lowest to the highest percentage. Early in the season, totals are small and percentages can change sharply with a single rain event.

2.2 Heat calendar 2026

Figure 5 shows each day of 2026 as the gap between the national mean temperature and the 1991–2020 normal for the same day. From 1 January to 18 October 2026, the mean gap is +1.40 °C; 87 days out of 291 exceeded the 90th percentile of the reference period and 4 exceeded its maximum. Over the last thirty days available, the mean gap is +2.6 °C.

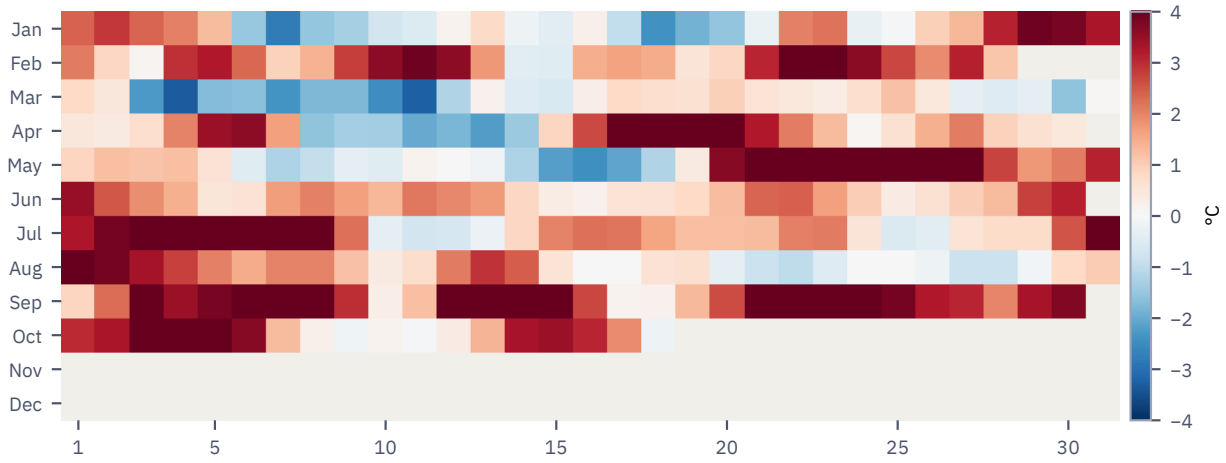


Figure 5: Daily gap between the national mean temperature and the 1991–2020 normal, 2026 (°C)
One cell per day (rows: months; columns: days). Daily normal computed over a ±7-day window. Grey cells: days not yet available. Source: Open-Meteo (ERA5 reanalysis), Observatory calculations.

2.3 Snow on the Atlas

Snow falling on the Atlas in winter feeds rivers and dams in spring. In the 2025/26 season, average fresh snowfall at the four monitored points reached 228 cm, 274 % of normal (83 cm), with 51 snow days against 20 on average. Since 1 September, the total is 0 cm (normal for the same date: 1 cm).

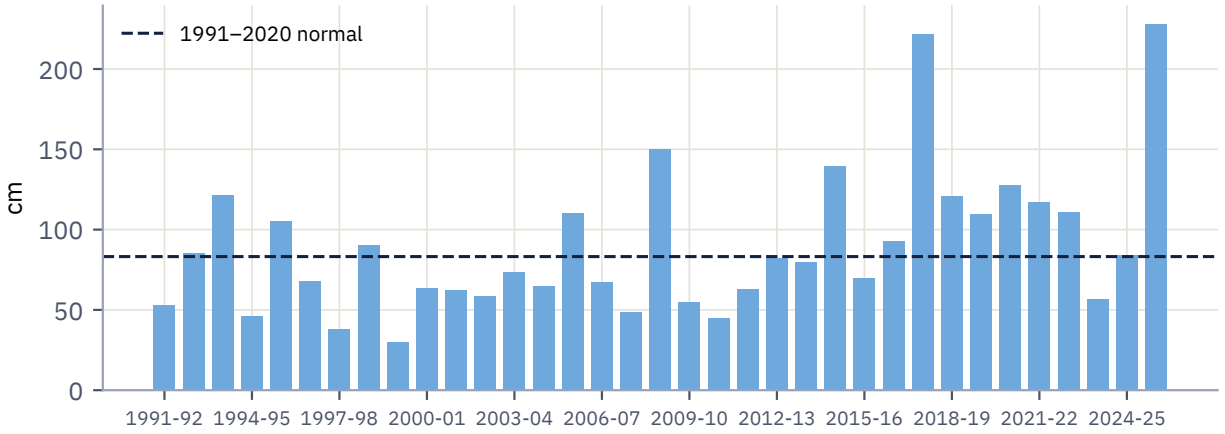


Figure 6: Snowfall by season, mean of the four Atlas points (cm)
Points: Ifrane, Jbel Ayachi, Imilchil, Oukaimeden. Grid cells of about 25 km: values are lower than snowfall on the summits and are mainly useful for comparing seasons. Snow day: at least 1 cm. Source: Open-Meteo (ERA5 reanalysis), Observatory calculations.

2.4 Dam reserves

According to the latest published situation, national dam filling stands at 65.9 % on 19 October 2026, about 11.2 billion m^3.

Source: Ministry of Equipment and Water, situation published on maadialna.ma; history compiled by the Observatory.

3 Coming heat, air, sea and seasonal outlook

3.1 Heat over the next seven days

The forecast of 23 October 2026 points to very hot days in 3 regions: Souss-Massa (2 days); Guelmim-Oued Noun (1 day); Dakhla-Oued Ed-Dahab (5 days, including at least three in a row). A very hot day is one when the forecast maximum temperature exceeds the 90^{th} percentile of the same month over 1991–2020; the comparison is indicative, as the forecast comes from a weather model and the threshold from the ERA5 reanalysis.

Source: Open-Meteo (weather forecasts); thresholds: Open-Meteo (ERA5 reanalysis), Observatory calculations.

3.2 Air quality and dust

At collection time, the European air quality index is fair in 8 regions, good in 2 regions, moderate in 1 region, poor in 1 region. Poor or worse air is forecast in 18 region-days over the following days.

Source: Copernicus Atmosphere Monitoring Service (CAMS), via Open-Meteo. Model estimates at each regional capital, not station measurements; European Air Quality Index classes.

3.3 Sea temperature

Table 3: Sea surface temperature off the coast, 22 October 2026

Point	Temperature (°C)	Change over 30 days (°C)	Gap with last year (°C)
Mediterranean (Al Hoceima)	20.7	−0.9	n/a
Atlantic (Tangier)	20.3	+0.8	n/a
Casablanca	21.2	−2.2	n/a
Agadir	21.2	+2.4	n/a
Laayoune	20.6	+0.2	n/a
Dakhla	21.5	+0.7	n/a

n/a: the Observatory's record is still shorter than one year. Source: Météo-France sea surface temperature analysis, via Open-Meteo.

3.4 Seasonal outlook

According to the seasonal forecast of 23 October 2026, 6 months out of 6 are expected to be warmer than the model's normal at national level, and 2 drier. These are forecasts, not measurements: they indicate a tendency whose reliability decreases with lead time.

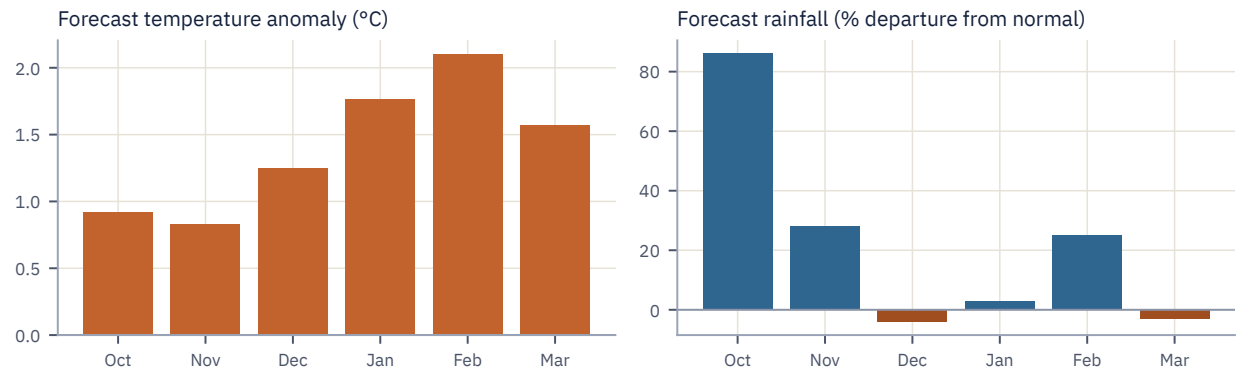


Figure 7: Seasonal forecast, national mean

Anomalies relative to the model's own climate (mean of its past forecasts for the same month). Unweighted mean of regional capitals. Source: ECMWF SEAS5, via Open-Meteo, Observatory calculations.

4 Climate risk and financial stress indices

4.1 Changes since 1998

The CRI summarises temperature, precipitation and the carbon intensity of activity; the FSI aggregates eight variables covering the banking sector, the stock market, public finances and the external sector. Both indices are built by weighted principal component analysis and rescaled to 0–100 relative to the period 1998–2025. The three highest FSI values are observed in 2012 (100.0), 2011 (89.4), 2019 (87.8).

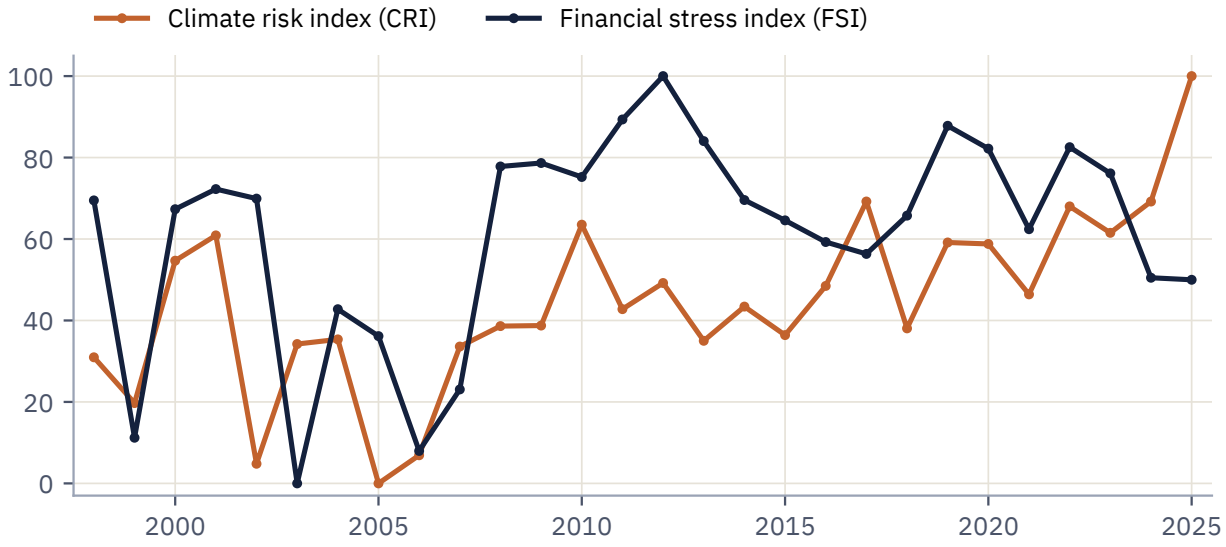


Figure 8: Climate risk index (CRI) and financial stress index (FSI), 1998–2025

Scale 0–100 relative to the reference period. Source: Observatory calculations; method: El Khlifi et al. (2026).

4.2 Reading the CRI level in 2025

The maximum CRI value in 2025 calls for a cautious reading. The index combines the first principal component and the absolute value of the second, which captures atypical deviations whatever their direction. A year with exceptionally abundant rainfall therefore raises the index just as a very dry year does. In 2025, the atypical deviation component contributes 46.4 points (46 % of the value),

against 53.6 points for the main part; the variant based on the first component alone stands at 80.9 (figure 9). The high level of the index thus reflects a climatically unusual year rather than an exceptional drought.

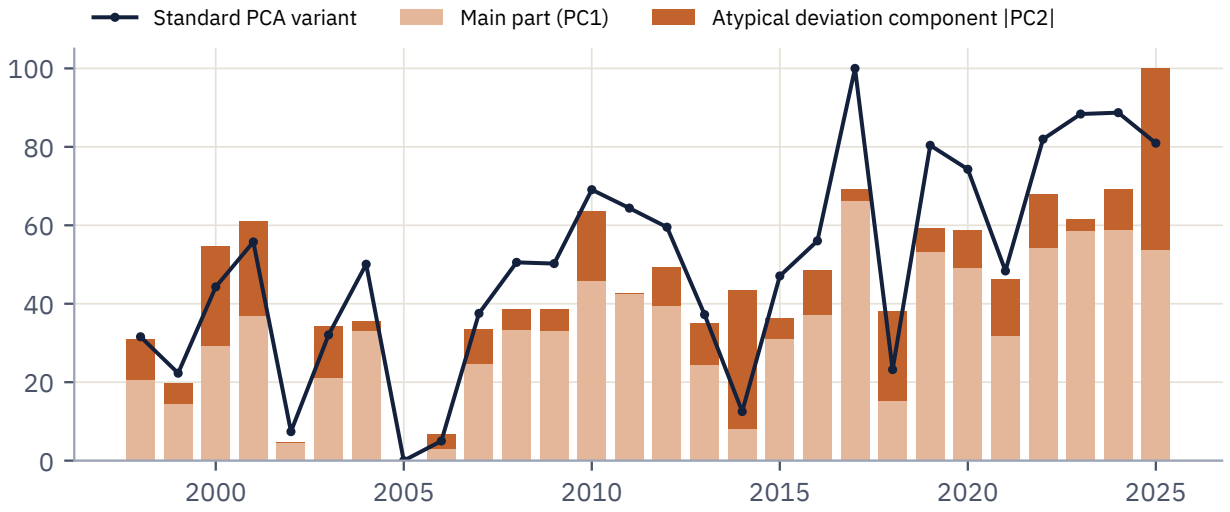


Figure 9: CRI decomposition and standard PCA variant
Source: Observatory calculations.

5 Financial stress index forecast

The one-year-ahead FSI forecast compares five models: a naive model, which carries forward the previous year's value; a linear regression on the previous year's FSI and CRI; a support vector regression (SVR) with a Gaussian kernel; a random forest and gradient boosting. All hyperparameters are set in advance. The evaluation is out of sample, with an expanding window, over 17 years (2009–2026): each year is forecast using only earlier data. Accuracy is compared with the naive model using the Diebold and Mariano (1995) test, with the Harvey et al. (1997) small-sample correction.

Table 4: Out-of-sample accuracy and 2026 forecast

Model	RMSE	MAE	DM vs naive (p)	2026 forecast [P10; P90]
Naive (previous year's value)	13.2	10.7	ref.	50.0 [32.5 ; 66.5]
Linear regression (OLS)	24.5	20.5	−2.59 (0.020)	99.4 [67.6 ; 134.0]
SVR (RBF kernel)	19.8	16.5	−1.64 (0.121)	67.0 [52.3 ; 99.1]
Random forest (500 trees)	16.2	13.1	−1.34 (0.201)	57.6 [42.3 ; 83.4]
Gradient boosting (200 trees)	19.4	16.2	−1.58 (0.134)	53.1 [35.5 ; 79.2]

RMSE, MAE: errors in FSI points. DM: corrected Diebold-Mariano statistic (negative value: model less accurate than the naive one). Interval: 10th and 90th percentiles of the model's out-of-sample errors. In bold: retained model.

The lowest error is that of the naive model (RMSE of 13.2 points), ahead of the random forest (16.2), gradient boosting (19.4), the SVR (19.8), the linear regression (24.5). The linear regression is significantly less accurate than the naive model ($p = 0.020$). The SVR is not significantly different from the naive model ($p = 0.121$). The random forest is not significantly different from the naive model ($p = 0.201$). Gradient boosting is not significantly different from the naive model ($p = 0.134$). On such a short annual sample, the available information therefore does not improve the

FSI forecast beyond its persistence. The retained forecast for 2026 is 50.0, within an interval of [32.5; 66.5].

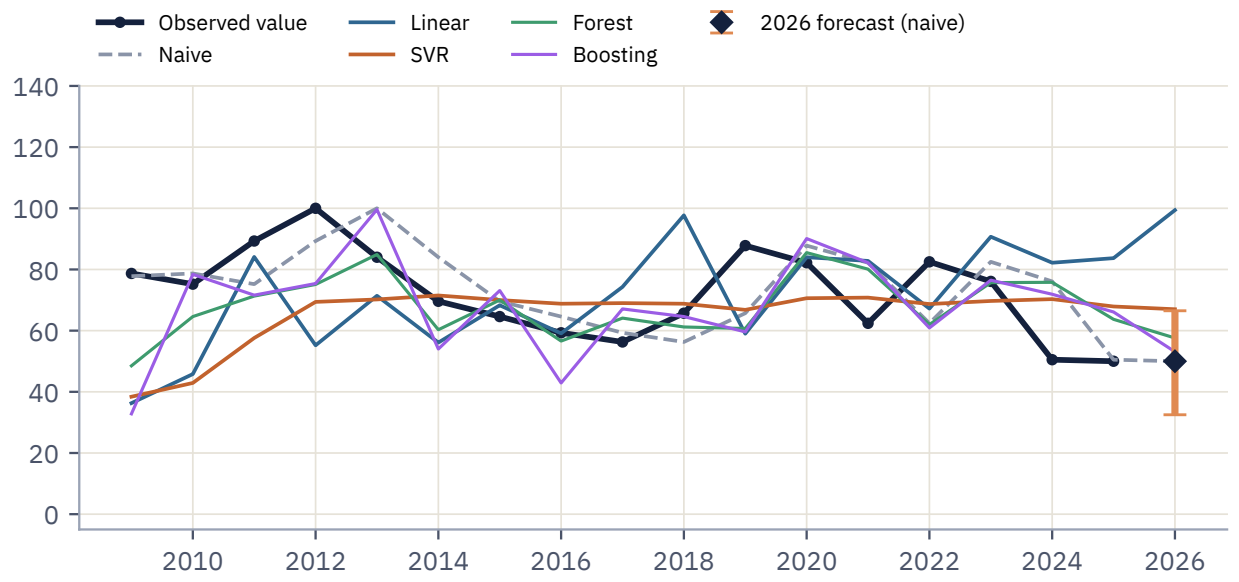


Figure 10: Out-of-sample forecasts and observed FSI values
Source: Observatory calculations.

6 Advanced analyses and projections

6.1 What a machine learning model relies on

A random forest (500 trees, hyperparameters set in advance) reproduces each year's FSI from five variables: the previous year's FSI, the temperature anomaly, the year's drought (December SPEI-12), very hot days and agricultural value added growth. Exactly computed Shapley values split the gap between the model value and its average level among these variables. Over 1999–2025, the random forest relies first on "Very hot days in the year" (43.8% of contributions) then on "Previous year's FSI" (33.2%). It reproduces the past with an R^2 of 0.58, but its out-of-sample error (RMSE of 22.4 points over 17 years) is higher than the naive model's (13.2). For 2025, the model value (56.7) departs from the average level (61.1) mainly through Previous year's FSI (−7.7) and Very hot days in the year (+4.1). These contributions describe how the model works; they establish no causal effect, and a variable that rises over time may capture a common trend.

6.2 Unusual climate months

An isolation forest compares each month since 1991 with the other months in the same region, using the temperature anomaly, SPEI-1, SPEI-3 and very hot days. In September 2026, 6 regional series are among the 3% most unusual months since 1991: Laayoune-Sakia El Hamra (many very hot days); Fez-Meknes (many very hot days); Guelmim-Oued Noun (temperature far above normal); Tanger-Tetouan-Al Hoceima (many very hot days); national average (many very hot days); Marrakesh-Safi (many very hot days). The variable cited is the one furthest from its usual level.

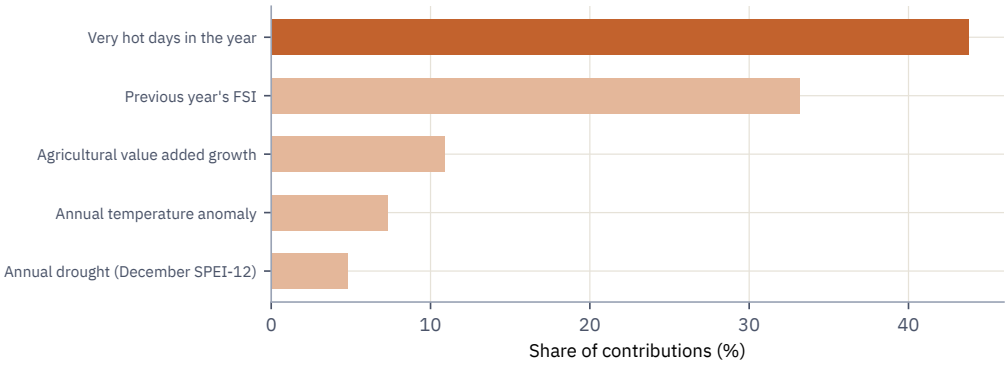


Figure 11: Share of each variable in Shapley contributions (mean absolute value)
Source: Observatory calculations (scikit-learn); Open-Meteo (ERA5); World Bank.

7 Transmission of climate shocks: estimation results

The results below come from estimations over 1999–2025 (27 annual observations): a five-variable VAR(1), with the CRI ordered first, and equation-by-equation quantile regressions. They are reported as they are, without re-estimation.

In the VAR, the coefficient of the lagged CRI in the FSI equation is 0.624 ($p = 0.007$). The Granger (1969) test concludes that the CRI precedes the FSI ($F = 6.75$, $p = 0.016$), confirmed by the Toda and Yamamoto (1995) procedure ($\chi^2 = 8.45$, $p = 0.012$); the reverse relationship is not significant ($\chi^2 = 0.11$, $p = 0.742$). According to this coefficient, a one-standard- deviation shock to the CRI (21.9 points) is associated with an increase of about 13.7 FSI points the following year. The orthogonalised impulse response (figure 12) is statistically significant only at the one-year horizon (15.9 points); at ten years, the CRI explains 45.9 % of the FSI forecast error variance.

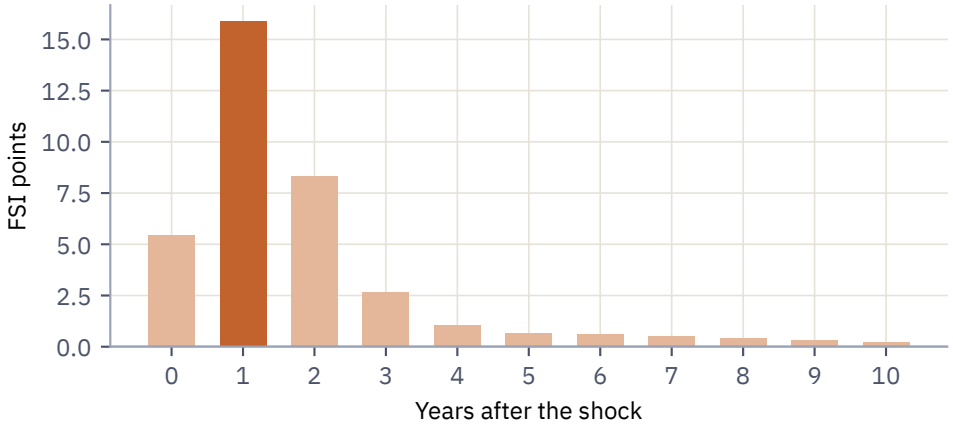


Figure 12: FSI response to a one-standard-deviation shock to the CRI
Orthogonalised shock (Cholesky decomposition). Dark bar: only horizon where the response is significant at the 5 % level.

At the quantiles, the confidence intervals include zero and the test of equal coefficients across quantiles does not reject equality ($p = 0.496$). The hypothesis of a stronger effect in periods of high stress is therefore not supported by these data. Taken together, these results establish predictive precedence of climate risk over financial stress; they do not allow a causal conclusion.

Table 5: Coefficient of the lagged CRI in the FSI equation, by quantile

Estimation	Coefficient	95 % confidence interval	p-value
Quantile 0.2	0.667	[−0.252 ; 1.288]	0.180
Quantile 0.5	0.687	[−0.516 ; 1.369]	0.358
Quantile 0.8	−0.027	[−0.772 ; 1.719]	0.922
Quantile 0.9	−0.233	[−0.878 ; 1.922]	0.860
VAR (mean)	0.624	[0.141 ; 1.108]	0.007

Quantile regressions: bootstrap intervals and p-values (1,000 draws). VAR: asymptotic interval and p-value.

8 Morocco compared with its neighbours

Figure 13 places Morocco relative to Algeria, Tunisia, Egypt and Spain on ten annual World Bank indicators, economic and sustainable development (water and energy). Differences between countries also reflect different economic structures and national statistical methods.

Table 6: Latest available value by country

Indicator	Morocco	Algeria	Tunisia	Egypt	Spain
GDP growth (%)	4.6^{25}	3.8^{25}	2.5^{25}	4.4^{25}	2.8^{25}
Agriculture value added growth (%)	3.7^{25}	5.2^{25}	10.3^{25}	2.8^{25}	1.2^{25}
Agriculture value added (% of GDP)	10.5^{25}	14.5^{25}	10.3^{25}	16.6^{25}	2.7^{25}
Domestic credit to private sector (% of GDP)	79.2^{25}	19.6^{25}	57.7^{25}	25.8^{25}	74.2^{24}
Inflation, consumer prices (%)	0.7^{25}	1.4^{25}	5.2^{25}	14.1^{25}	2.7^{25}
Personal remittances (% of GDP)	7.5^{25}	0.6^{25}	6.7^{25}	11.4^{25}	0.4^{25}
Renewable internal freshwater resources per capita (m^3)	776.9^{22}	247.3^{22}	346.1^{22}	8.9^{22}	$2{,}327.0^{22}$
Water stress: freshwater withdrawal (% of available resources)	50.8^{22}	144.8^{22}	98.1^{22}	141.2^{22}	43.3^{22}
Renewable electricity output (% of total)	19.3^{21}	0.9^{21}	2.8^{21}	12.2^{21}	47.0^{21}
Renewable energy (% of final energy consumption)	10.9^{21}	0.1^{21}	11.6^{21}	6.1^{21}	19.0^{21}

Superscript: year of the value (last two digits). Source: World Bank, World Development Indicators.

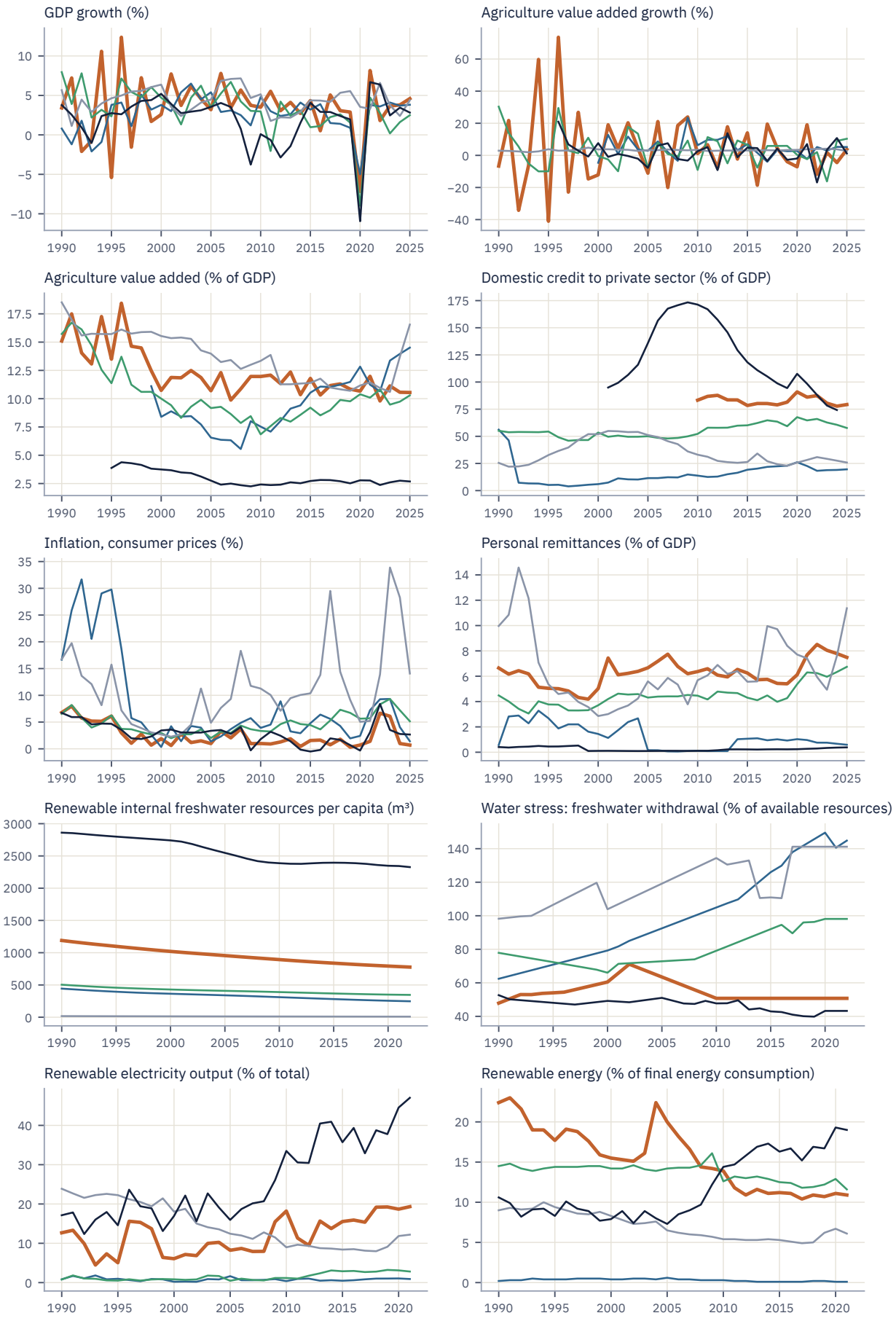


Figure 13: Economic and sustainable development indicators compared

Source: World Bank, World Development Indicators.

9 Methodology and limitations

- **Climate data.** Daily series from the ERA5 reanalysis (Hersbach et al., 2020) distributed by the Open-Meteo historical archive, at the representative point (capital) of each of the twelve regions, since 1991. National values are the unweighted mean of the available regional points; they do not account for the area of the regions.
- **Indicators.** Anomalies and precipitation relative to 1991–2020 monthly normals. SPEI at 3 and 12 months fitted with a three-parameter log-logistic distribution for each calendar month, falling back on a normal distribution when the fit fails in the dry season. Hot days defined by the 90th percentile of the maximum temperature of the same month.
- **Water and heat.** Farming season: daily cumulative precipitation since 1 September, compared with the 1991/92–2019/20 seasons. Snow: ERA5 snowfall at four Atlas points. Dams: latest published national situation. Heat forecasts, air quality, sea temperature and seasonal forecasts: model products distributed by Open-Meteo, presented as indications rather than measurements.
- **Composite indices.** Principal component analysis on robustly scaled variables, weighted combination of the first component and the absolute value of the second, normalisation to 0–100. Parameters are estimated over the reference period and then frozen; a new year is computed only if all its components are available.
- **Scope of the results.** The composite indices rely on about thirty annual observations; the tests and forecasts derived from them carry substantial uncertainty. The relationships presented are associations or predictive precedence.

Glossary

SPEI Standardised drought index: departure of the water balance (precipitation minus evapotranspiration) from the normal for the same period. Below -1: moderate drought; below -1.5: severe; below -2: extreme. The number 3 or 12 gives the number of months accumulated.

Temperature anomaly Gap between the observed mean temperature and the mean of the same month over 1991–2020.

Very hot day Day when the maximum temperature exceeds the 90th percentile of the same month over 1991–2020.

Farming season Period from 1 September to 31 August, matching the cycle of rain-fed crops in Morocco.

European Air Quality Index Index combining particle and gas concentrations; classes from good to extremely poor.

CRI Annual climate risk index (temperature, precipitation, carbon intensity), scale 0–100.

FSI Annual financial stress index (banks, stock market, public finances, external sector), scale 0–100; a high value signals greater stress.

Predictive precedence The past of one variable improves the forecast of another; this does not establish a cause-and-effect link.

References

Diebold, F. X. and Mariano, R. S. (1995). Comparing predictive accuracy. *Journal of Business & Economic Statistics*, 13(3), 253–263.

El Khlifi, I., Drissi Bakhkhat, M. and Madkour, J. (2026). Climate risks and financial stability in Morocco: An emerging challenge for sustainable development. *European Journal of Government and Economics*, 15(1), 163–193. https://doi.org/10.17979/ejge.2026.15.1.12680

Granger, C. W. J. (1969). Investigating causal relations by econometric models and cross-spectral methods. *Econometrica*, 37(3), 424–438.

Harvey, D., Leybourne, S. and Newbold, P. (1997). Testing the equality of prediction mean squared errors. *International Journal of Forecasting*, 13(2), 281–291.

Hersbach, H. et al. (2020). The ERA5 global reanalysis. *Quarterly Journal of the Royal Meteorological Society*, 146(730), 1999–2049.

Toda, H. Y. and Yamamoto, T. (1995). Statistical inference in vector autoregressions with possibly integrated processes. *Journal of Econometrics*, 66(1–2), 225–250.

Vicente-Serrano, S. M., Beguería, S. and López-Moreno, J. I. (2010). A multiscalar drought index sensitive to global warming: The standardized precipitation evapotranspiration index. *Journal of Climate*, 23(7), 1696–1718.

Data: Open-Meteo, Historical Weather, Forecast, Air Quality, Marine and Seasonal Forecast APIs (https://open-meteo.com); Ministry of Equipment and Water, dam situation (https://www.maadialna.ma); World Bank, World Development Indicators (https://data.worldbank.org); OpenStreetMap contributors (ODbL).